Low Energy Electron Diffraction from Ag(001) and Ag(111) surfaces

Jayanta Das*

*Dept. of Physics, Panchakot Mahavidyalaya, Purulia, W.B. -723121, India; email: jayanta.sinp@gmail.com

Abstract

Electron diffraction experiments were performed on the surfaces of Ag(001) and Ag(111) single crystals. The incident low-energy (20-200 eV) electrons were scattered by the crystallographic planes of the samples and diffraction patterns were produced on the phosphor screen. The diffraction experiments were performed inside the ultra high vacuum chambers. The surface symmetry, ordering and orientations were identified from the corresponding diffraction patterns. The scattered electrons produced square and hexagonal diffraction patterns, respectively for Ag(001) and Ag(111) surfaces. As the incident beam energy is gradually increased, higher order diffraction spots entered into the field-of-view. The surface brillouin zones of the corresponding crystals and the high-symmetry directions were identified from the diffraction patterns. Moreover, the basic functions of LEED and optimizations of various parameters such as sample position, Wehnelt voltage were explained.

Keywords: Low Energy Electron Diffraction, Surface Symmetry, Brillouin Zone

Introduction

The diffraction of electrons by metallic crystals were first reported by Davisson and Germer [1] on 1927. Being a milestone for understanding the quantum mechanical wave-particle duality, their experimental result was the threshold of electron diffraction physics. Initially, Low Energy Electron Diffraction (LEED) was used merely to monitor the surface conditions [2,3]. With the technological advancement and ability to achieve ultra-high vacuum, the low energy electrons, with their extreme surface sensitivity, became a useful tool to explore the minute details of crystal surfaces. The crystalline symmetry and shape of the surface unit cells, symmetry directions and orientations could be characterized from LEED studies. Moreover, the details of surface adsorptions [4], two-dimensional surface phase transitions, reconstructions [5], defects [6], mosaic formations [7], and step-terrace structures [8] *etc.* could successfully be investigated by LEED. In addition to that, the structural specifications [9], e.g. the atomic positions within the unit cells of the crystals, could also be determined from the LEED spot intensities (I) plotted as a function of incident beam energies (V) in association with theoretical calculations [10,11].

In this article, the observation of LEED patterns from Ag(001) and Ag(111) crystal faces are reported for various incident electron beam energies. The Ag single crystal has *fcc* lattice structure while the surface unit cells on (001) and (111) planes are of square and hexagonal symmetry, respectively. Our LEED experiments show that the diffracted electrons from Ag(001) surface produce square patterns whereas the Ag(111) surface scatters electrons to produce hexagonal LEED pattern on

the screen. With increasing the incident electron energy, higher order diffraction spots enter into the LEED screen while symmetries of the reciprocal unit cells remain invariant. LEED pattern represents the two-dimensional reciprocal lattice of the crystal surface. The primitive unit cells within the first order diffraction patterns *i.e.* the First Surface Brillouin Zones (FSBZ) are demonstrated and the corresponding high symmetry directions are indicated accordingly.

Technical details

Both crystals, Ag(001) and Ag(111), were prepared and cleaned *via* multiple cycles of Ar^+ ion sputtering (Energy: 700 eV, Beam current=5 mA, Duration: 30 min) followed by annealing at 673 K for 30 min. In the sputtering process the incident high energy Ar^+ ions dig up and expose the shallow atomic layers to vacuum through removal of the top surface layers. The collisional impacts ruptures the surface crystalline order. The disordered surface could be healed *via* annealing of the sample at elevated temperatures to achieve good quality surface ordering.

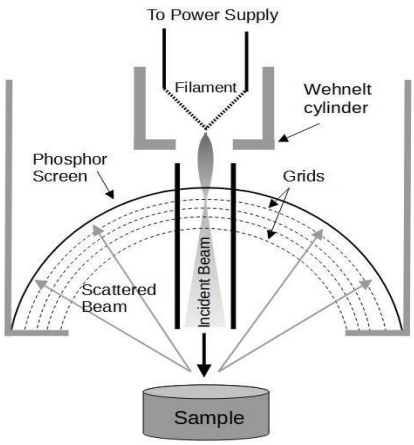

Figure 1: Schematic diagram of a LEED apparatus

Within the UHV chamber with base pressure 1×10^{-10} mbar, experiments were performed on clean Ag (001) and Ag(111) crystals using a four-grid LEED-apparatus. The schematic diagram of a LEED apparatus is shown in figure 1. Before collection of the actual experimental data, the apparatus is prepared and calibrated for best performance. The LEED filament must be well-degassed so that the UHV chamber pressure could be maintained during experiments. In general a thoriated-tungsten filament is used as cathode that emits electrons upon heating. These electrons are accelerated by a variable voltage to focus on the sample surface, where they are diffracted and traverse back in the vacuum toward the fluorescent screen. The sample position is optimized to keep the polished surface exactly at the center of the curved (part of a spherical) surface of the screen. To obtain the best vertical position (z) of the sample, LEED experiments were performed for various sample distances, keeping the Wehnelt voltage fixed at a reasonable value. The average radial intensity profiles of the LEED spots were measured for each z-position. In figure 2, the radial intensities of the LEED spots are plotted against the radial (pixel) distances. A variation of the HWHM (Half Width at Half-

Maxima) of the profiles with z-positions could be observed. The minimum HWHM at z=18 sample manipulator position corresponds to the sharpest LEED spots. Therefore, this position could be assigned as the center of the spherical phosphor screen.

The Wehnelt voltage [12] acts as an electrostatic lens to focus the incident electron beam. Therefore, a suitably chosen voltage helps to obtain narrowest electron beam from the gun and therefore, sharpest diffraction spots from the samples. To optimize this voltage the sample is kept at z=18 mm manipulator position. The sharpness of the LEED spots are monitored for various Wehnelt voltages. A plot of the LEED spot radial intensity profiles for different Wehnelt voltages are shown in figure 3. The minimum HWHM is obtained at 53 V which ensures

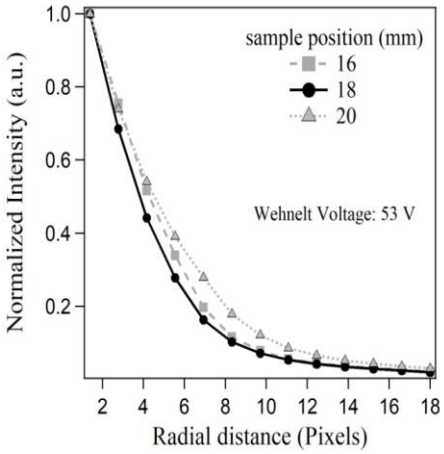

Figure 2: Radial intensity profile of LEED spot with sample position variation.

the narrowest pencil of electron beam from the gun. In general, the Wehnelt cylinder is kept at a negative bias with respect to the emitter. A typical beam size is of the order of 1 mm^2.

The secondary electrons and also the inelastically scattered electrons can be kept away from the screen by applying a negative voltage to the suppressor grids. A set of four gold coated molybdenum grids at different places in front of the fluorescent screen serves as energy filter. These grids prevent the access of low energy secondary electrons to the detection area, where the Bragg's diffraction spots could be observed. This reduces the LEED pattern background intensity. During the experiment, the low energy electrons (10-200 eV) from the electron gun fall on the crystal surfaces and are scattered by various crystal planes. The elastically scattered electrons are detected on a hemispherical phosphor screen kept at high (4-5 kV) potential. A Peltier-cooled 12-bit charged coupled device (CCD) camera with exposure control facility was used to capture the LEED patterns for various beam energies.

Experimental Results

The low energy electrons are extremely surface sensitive (first 2-3 atomic layers) and they have coherence length upto several hundred Angstroms (Å). Hence, they probe the long range atomic ordering at the surface.

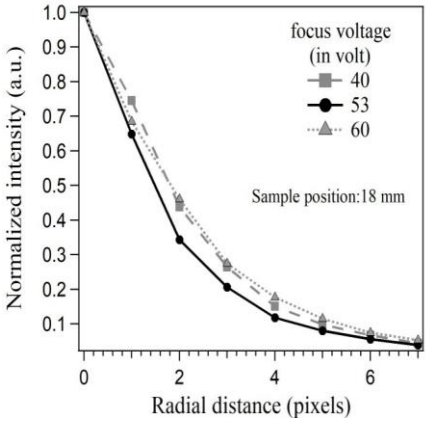

Figure 3: Radial intensity profile of LEED spot with Wehnelt voltage variation.

For the case of a good quality ordered surface the diffraction spots are sharper and smaller. In figures 4 (a) and (b), the LEED patterns from Ag(001) crystal are shown for beam energies 53 eV and 144 eV, respectively. The images are presented with inverted contrast for better visualization of diffraction spots. At 53 eV, the first order diffraction spots (1,0), (-1,0), (0,1), and (0,-1) are visible.

The back-scattered beam (0,0) is shadowed by the electron gun at the center of the image. At 144 eV beam energy, higher order diffraction spots enter into the field-of-view. With the increase of incident beam energy the Ewald sphere [13] radius increases and therefore, more Bragg rods cross the sphere. As a result, higher order LEED spots appear on the screen. However, in both figures 4(a) and (b), the reciprocal unit-cells have

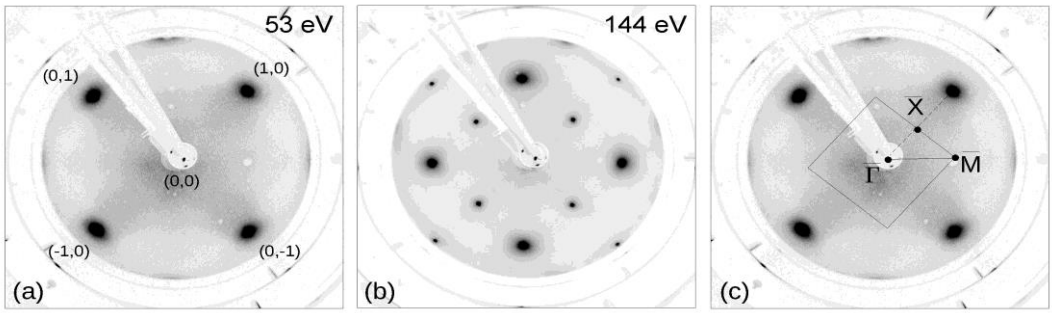

Figure 4: LEED patterns from Ag(001) sample. Beam energy (a) 53 eV (b) 144 eV. The square SBZ is shown in (c) with symmetry points $\bar{\Gamma}$, $\bar{M}$ and $\bar{X}$.

square symmetry which implies square unit cell on the Ag(001) surface. In figure 4(c), the Wigner-Seitz cell (square with continuous boundary) is shown. The central LEED spot (0,0) is connected to its four nearest neighbour spots. One such connection is demonstrated in figure 4(c) by dashed straight line. Four perpendicular bisectors drawn over these connecting lines enclose a region/area of the reciprocal space. This enclosed region is the Wigner-Seitz cell which, within the reciprocal space, is also termed as the First Surface Brillouin Zone (FSBZ). In figure 4(c), the FSBZ has square symmetry the center of which is $\bar{\Gamma}$point. The mid-points of each side of the BZ are $\bar{X}$while the corner points are indicated as $\bar{M}$.

Figures 5(a) and (b) represent the LEED patterns from Ag(111) surface for incident electron energies 55 eV and 120 eV, respectively. The LEED symmetry implies hexagonal atomic arrangement on the Ag(111) surface. In figure 5(c), the corresponding FSBZ and the symmetry points $\bar{\Gamma}$, $\bar{K}$and $\bar{M}$are indicated accordingly.

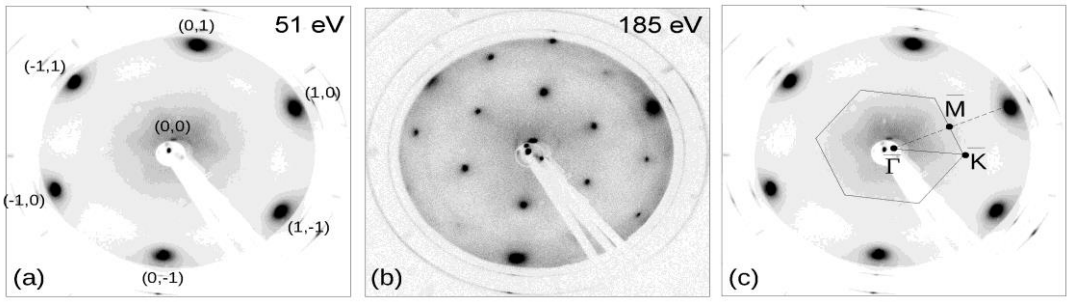

Figure 5: LEED patterns from Ag(111) sample. Beam energy (a) 51 eV (b) 185 eV. The square SBZ is shown in (c) with symmetry points $\bar{\Gamma}$, $\bar{K}$ and $\bar{M}$.

Conclusion

Low energy electrons were diffracted by Ag(001) and Ag(111) single crystal surfaces to produce diffraction patterns with square and hexagonal symmetry, respectively. The LEED patterns were collected for various incident beam energies. The atomic arrangements on the surfaces of the crystals could be predicted from the LEED patterns which represent the reciprocal of surface lattice. The Wigner-Seitz cells, considered on the LEED, represent the SBZs of the corresponding crystals. The high-symmetry points on the SBZ are indicated accordingly while $\bar{\Gamma}$at the zone center represents the point of highest symmetry. The azimuthal orientations of the crystal surfaces could be estimated from these studies which are useful for directional electron-spectroscopic studies.

Acknowledgement

The author acknowledges the ARPES laboratory of Surface Physics and Material Science division, Saha Institute of Nuclear Physics, Kolkata, India for technical help and support.

References

1. Davisson, C. and Germer, L. H., (1927). Diffraction of electrons by a crystal of Nickel. *Nature*. **119**: 558-560.
2. Scheibner, E. J., Germer, L. H. and Hartman, C. D. (1960). Apparatus for direct observation of low energy electron diffraction pattern. *Review of Scientific Instruments*. **31**: 112.
3. Lander, J. J., Unterwald, F. and Morrison, J. (1962). Improved design and method of operation of low energy electron diffraction equipment. *Review of Scientific Instruments*. **33**: 784.
4. Wander, A., Van Hove, M.A. and Somorjai, G. A. (1991). Molecule-induced displacive reconstruction in a substrate surface: Ethylidyne adsorbed on Rh(111) studied by low-energy-electron diffraction, *Physical Review Letter*. **67**: 626-628.
5. Liew, Y.F. and Wang, G.C. (1991). High resolution low energy electron diffraction characterization of Au(001) surfaces, *Surface Science*. **227**: 190-196.

6. Wollschl*ä*ger, J. and Henzler, M. (1989). Defects at the Si(111)/SiO_2 interface investigated with low-energy electron diffraction. *Physical Review B*. **39**: 6052-6059.
7. Welkie, D. G. and Lagally, M. G. (1980). Low-energy electron diffraction study of the surface defect structure of Ag(111) epitaxially grown on mica. *Journal of Vacuum Science Technology*. **17**: 453.
8. De la Figuera, J., Puerta, J.M., Cerda, J.I., Gabaly, F. El and McCarty, K.F. (2006). Determining the structure of Ru(0001) from low energy electron diffraction of a single terrace. *Surface Science.* **600(9)**: L105-L109.
9. Reichelt, R., G*ü*nther, S. and Wintterlin, J. (2007). Low energy electron diffraction and low energy electron microscopy microspot I/V analysis of the (4x4) O structure on Ag(111): Surface oxide or reconstruction? *The Journal of Chemical Physics.* **127**: 134706.
10. Pendry, J. B. (1974). *Low Energy Electron Diffraction*, Academic Press, New York.
11. Van Hove, M. A., Weinberg, W. H. and Chan, C.M. (1986). *Low-Energy Electron Diffraction Experiment, Theory and Surface Structure Determination*, Springer-Verlag, Berlin.
12. Fleming, A. (1934). On the history and development of the thermionic valve. *Journal of Scientific Instruments*, **11**: 44.
13. Ewald, P.P. (1969). Introduction to the dynamical theory of X-ray diffraction. *Acta Crystallographia Section A*, **25 (1)**: 103-108.